THE JOURNAL OF BIOLOGICAL CHEMISTRY
Vol. 278, No. 21, Issue of May 23, pp. 18761–18766, 2003

Printed in U.S.A.

Direct Detection of Fe(IV)=O Intermediates in the Cytochrome aa_3 Oxidase from *Paracoccus denitrificans*/H_2O_2 Reaction*

Received for publication, November 22, 2002, and in revised form, February 25, 2003
Published, JBC Papers in Press, March 13, 2003, DOI 10.1074/jbc.M211925200

Eftychia Pinakoulaki‡§, Ute Pfitzner¶, Bernd Ludwig¶, and Constantinos Varotsis‡‖

From the ‡Department of Chemistry, University of Crete, 71409 Heraklion, Crete, Greece and the ¶Institute of Biochemistry, Biozentrum, Johann Wolfgang Goethe-Universität, Marie-Curie-Str. 9, D-60439 Frankfurt/Main, Germany

We report the first evidence for the formation of the "607- and 580-nm forms" in the cytochrome oxidase aa_3/H_2O_2 reaction without the involvement of tyrosine 280. The pK_a of the 607–580-nm transition is 7.5. The 607-nm form is also formed in the mixed valence cytochrome oxidase/O_2 reaction in the absence of tyrosine 280. Steady-state resonance Raman characterization of the reaction products of both the wild-type and Y280H cytochrome aa_3 from *Paracoccus denitrificans* indicate the formation of six-coordinate low spin species, and do not support, in contrast to previous reports, the formation of a porphyrin π-cation radical. We observe three oxygen isotope-sensitive Raman bands in the oxidized wild-type aa_3/H_2O_2 reaction at 804, 790, and 358 cm^{-1}. The former two are assigned to the Fe(IV)=O stretching mode of the 607- and 580-nm forms, respectively. The 14 cm^{-1} frequency difference between the oxoferryl species is attributed to variations in the basicity of the proximal to heme a_3 His-411, induced by the oxoferryl conformations of the heme a_3-Cu_B pocket during the 607–580-nm transition. We suggest that the 804–790 cm^{-1} oxoferryl transition triggers distal conformational changes that are subsequently communicated to the proximal His-411 heme a_3 site. The 358 cm^{-1} mode has been found for the first time to accumulate with the 804 cm^{-1} mode in the peroxide reaction. These results indicate that the mechanism of oxygen reduction must be reexamined.

Establishing the structural and functional properties of the binuclear center in cytochrome *c* oxidase (CcO)[1] is essential in understanding the linkage of the structural features with the structure of transient O_2 intermediates that are important for the protein to function as a redox-linked proton pump (1–6). CcO contains a homo-dinuclear Cu_A center, one low spin heme a, and a high spin heme a_3-Cu_B binuclear center where the reduction of dioxygen to H_2O takes place (1–15). One of the unique properties of the binuclear heme a_3-Cu_B center that were determined by the crystal structures of the bovine, the *Paracoccus denitrificans*, and the *Thermus thermophilus* heme copper oxidases is the Tyr-280–His-276 (*P. denitrificans* numbering) cross-linked structure (7–11). Tyr-280 is located at the end of the proton K-channel and is highly conserved among the heme copper oxidases. The suggestion that the O-O bond cleavage proceeds by concerted hydrogen atom transfer from the cross-linked His-Tyr species to produce the Fe(IV)=O/Cu_B^{2+}-His-Y$^{\bullet}$ species raises important issues as to the means by which the electron transfer to these transient species is regulated for conformational transitions that are required to occur in any pumping mechanism (13, 16).

The CcO/H_2O_2 reaction has been a conundrum and subject of debate for a number of years (17–28). The reaction serves as an alternative view of the peroxy ($2e^-$) oxidation level. The CcO/H_2O_2 reaction, monitored extensively by optical absorption, forms consecutively the 607- and 580-nm forms, and their formation is dependent on the concentration of substrate and pH. Importantly, both forms were first observed in mitochondria during the reversal of electron transfer from water to cytochrome *c* (29). Recent studies have suggested that at high pH, addition of stoichiometric amounts of H_2O_2 to oxidized enzyme leads to the formation of the 607-nm form having the Fe(IV)=O····HO-$Cu(II)_B$-Y$^{\bullet}$ structure, whereas the 580-nm form having the Fe(IV)=O $Cu(II)_B$-Y$^{\bullet}$ structure is the result of a single protonation of the former species (14). At low pH, the 580-nm form is also produced by addition of stoichiometric amounts of H_2O_2 to the enzyme (14). Addition of a second equivalent of H_2O_2 converts each of the above mentioned species to Fe(IV)=O Cu_B^{2+}-His-Y. On the other hand, it has been reported that the formation of the 580-nm form, but not that of the 607-nm form, results in a radical-like EPR signal (24). The involvement of Cu_B as the alternative electron source in the O-O cleavage process through its Cu_B(III) oxidation state has been suggested (25). Recently, the broad component of the EPR spectrum of H_2O_2-treated oxidized bovine CcO was attributed to a tryptophan cation radical exchange coupled to the oxoferryl Fe(IV)=O state of heme a_3, whereas the second observed signal to a porphyrin cation radical (28). In the later study, it was concluded that these EPR signals were not related to those demonstrating the presence of a tyrosine radical in the binuclear center (27) but were interpreted to arise from a tryptophan residue ~ 9 Å away from heme a_3.

Characterization of the Fe(IV)=O intermediates generated in the oxidized CcO/H_2O_2 reaction and their pH and H_2O_2 concentration dependence has been reported (21–23). It was demonstrated that under steady-state conditions, the peroxide reaction generates the 607- and 580-nm forms with 1 and 5 mM H_2O_2, respectively, and produces the same oxygen isotope-sensitive RR modes as those found for the transient intermediates in the O_2 reaction with CcO (30–40). In the pH 7.4–10 range, the population of the 607-nm form with a characteristic ν(Fe(IV)=O) mode at 804 cm^{-1} decreased at higher pH and at

* This work was supported by Alexander von Humboldt-Stiftung (to C. V. and B. L.), in part by the Greek Ministry of Education, and by Grant SFB 472 from the Deutsche Forschungsgemeinschaft (to B. L.). The costs of publication of this article were defrayed in part by the payment of page charges. This article must therefore be hereby marked "*advertisement*" in accordance with 18 U.S.C. Section 1734 solely to indicate this fact.

§ Recipient of a short term fellowship (ASTF 9480 from European Molecular Biology Organization).

‖ To whom correspondence should be addressed. Fax: 30-281-039-3601; E-mail: varotsis@edu.uoc.gr.

[1] The abbreviations used are: CcO, Cytochrome *c* oxidase; MV, mixed valence; RR, resonance Raman; MES, 4-morpholineethanesulfonic acid; CHES, 2-(cyclohexylamino)ethanesulfonic acid.

high concentrations of H_2O_2 (5 mM). Formation of the 580-nm form at non-saturating levels of H_2O_2 yields two more oxygen isotope-sensitive Raman modes at 785 and 355 cm^{-1}. The first disappears above pH 8.5 and has been assigned to a second Fe(IV)=O species; the second disappears at pH above 9.0 without significant changes in the absorption spectrum and has been attributed to a third oxoferryl species that is not related to either of the Fe(IV)=O species observed at 785 and 804 cm^{-1}.

Recently, we demonstrated that the stability of the binuclear center is not compromised in the Y280H mutant oxidase lacking the Tyr-280–His-276 cross-link since heme a_3 retains the same proximal environment, spin, and coordination state as in the wild-type enzyme in both oxidized and reduced states (41). As a result of the different experimental approaches in the oxidized CcO/H_2O_2 reaction, there is no consensus on the structure of either the 607- or the 580-nm forms. The relationship between the 804 cm^{-1} and/or the 790 cm^{-1} RR modes with that at 355 cm^{-1} is also essential for the clarification of the structure of each intermediate. In the work presented here, we report the formation of the 607- and 580-nm forms and their associated RR bands at 804, 790, and 358 cm^{-1} in the reaction of oxidized wild-type aa_3 from *P. denitrificans* with H_2O_2 under steady-state conditions at ambient temperatures. Our data indicate that in the pH 6.6–7.4 range, the ~580-nm form is produced with a characteristic oxygen-sensitive mode at 790 cm^{-1}. In the pH 7.7–8.1 range, however, we obtain a mixture of both forms and two oxygen-sensitive RR bands at 804 and 358 cm^{-1}. Following the H_2O_2 reaction for the Y280H mutant, we report the production of the 607- and 580-nm forms and demonstrate that Tyr-280 is obviously not involved in their formation. The mixed valence Y280H/O_2 reaction reveals similar characteristics of the mixed valence wild-type/O_2 reaction, which further confirms that the production of the 607-nm form occurs without the involvement of the Tyr-280 residue.

EXPERIMENTAL PROCEDURES

Wild-type and Y28H mutant CcO were purified from *P. denitrificans* according to published procedures (42, 43). The activity of isolated wild-type and mutant CcO has been reported (43). The samples were concentrated to 100–150 μM in a desired buffer (pH 6.6, MES; pH 7.4–8.1, HEPES; pH 9.5, CHES) containing 0.1% dodecyl β-D-maltoside and stored in liquid nitrogen until use. In the resonance Raman experiments, the enzyme solution and an H_2O_2 buffer solution were placed in separate syringes and driven through two eight-jet tangential Gibson type mixers in series with a syringe pump (44–48, 70). The exit port of the mixer was designed to allow the oxidase solution (50 μM after mixing) to flow through a rectangular 2-cm-long flow cell with an internal 0.2 × 0.1-mm cross-section. The time resolution is determined by the flow rate, the cell cross-sectional area and the spacing between the sample, and the probing 427-nm laser beam. With the flow rate and geometry used in the present investigation, we are able to vary the time from the mixer to the laser beam from 2 to 5 min. The resonance Raman spectra were acquired as described elsewhere (41). The power incident on the CcO sample was typically 5–6 milliwatt to avoid photoeffects of the sample by the incident laser light due to the low flow rate. H_2O_2 was purchased from Aldrich, and $H_2{}^{18}O_2$ was purchased from Icon. The optical absorbance spectra were recorded with a PerkinElmer Life Sciences Lamda 20 UV-visible spectrometer.

RESULTS

Fig. 1*A* shows the optical difference spectra upon reacting 6 μM oxidized CcO with 3 mM H_2O_2 minus oxidized CcO at pH 7.7 at the indicated times. The spectra are characterized by two peaks at 586 and 610 nm. The progression of changes in the difference spectra indicates that maximum occupancy occurs at 10 min in the reaction. The difference spectra are similar to those obtained for the reaction of oxidized mammalian and *Rb. sphaeroides* aa_3-type oxidase with H_2O_2 (49, 50). When this experiment is conducted with the Y280H mutant, the difference spectrum (*trace b*) is slightly changed with the maxima at

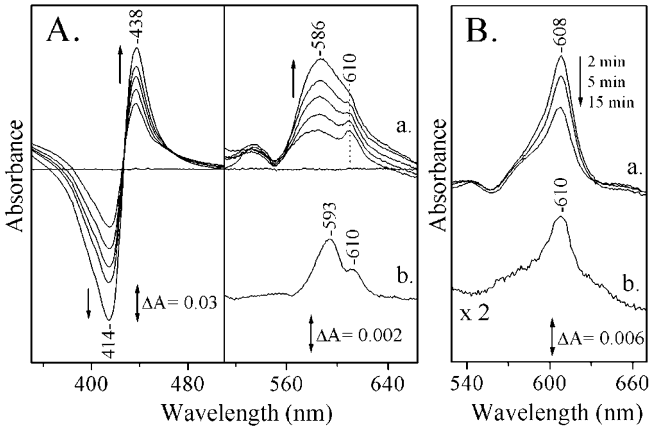

FIG. 1. **Optical absorption difference spectra.** *A*, optical absorption difference spectra showing the H_2O_2 reaction products minus the resting form of the wild-type *cytochrome aa3* from *P. denitrificans* (*trace a*) at 2, 3, 4, 5, and 10 min subsequent to mixing and the Y280H mutant (*trace b*) at 2 min subsequent to mixing; sample concentration, 6 μM; [H_2O_2] = 3 mM. The pH in both reactions was 7.7. *B*, the optical absorption difference spectra of the reaction products by direct mixing of O_2 with CO-MV wild-type (*trace a*) and Y280H enzymes (*trace b*) minus the resting form of the enzymes at 2 min subsequent to mixing and pH 8. The concentration of the enzymes was 5 μM, and the path length of the cell was 1 cm.

593 and 610 nm. The 610-nm form in both the wild-type and mutant enzyme indicates that its production is independent of the cross-link Tyr-280–His-276 structure. Mixing of oxygen with the CO-bound MV oxidase yields long-lived oxygenated intermediate(s) that occur after the decay of the oxy-intermediate (41, 50–52). The visible region optical absorption spectra of the wild-type and the Y280H oxygenated species formed this way are shown in Fig. 1*B*. The time evolution for the decay of the 608-nm form (*trace a*) formed in the wild-type MV/O_2 reaction is similar to that reported by others for the mammalian aa_3 MV/O_2 reaction (53). Moreover, the difference spectrum (MV-CO/O_2 minus oxidized) of the Y280H enzyme shown in Fig. 1*B* (*trace b*) displays a maximum at 608 nm, albeit with decreased absorbance, which is similar to that of the wild type. If the 608-nm form we detect in the Y280H MV/O_2 reactions has the same structure as that obtained from the oxidized wild-type and mutant enzyme in their respective reactions with H_2O_2, then the contribution of the covalently linked tyrosine to its formation is minimal.

Fig. 2 shows the pH dependence of the 610- and 586-nm forms. The former is more populated at pH values above 7.7 but is replaced by the 586-nm form as the pH decreases. The effect of pH on the decay of the 610–586-nm form, shown in the *inset*, indicates that the transition is controlled by a group with a pK_a of 7.5. Since H_2O_2 is fully protonated in the pH range 5–8.5, we suggest that the protonation state of a residue in the binuclear moiety controls the reaction product. When the group is protonated, the reaction yields the 586-nm form, and when it is deprotonated, the reaction yields the 610-nm form. The 610-nm form weakly absorbs at pH 6.6 and 7.4, and only the 586-nm form is apparent in the spectrum, whereas at pH 7.7–8.1, both forms are present. The accelerated at low pH conversion of the 610- to the 586-nm form, cannot be reversed by restoring the initial pH.

Fig. 3 shows the high frequency RR spectra of oxidized enzyme and those of the reaction intermediates with H_2O_2 in the pH 6.6–9.6 range at 2 min subsequent to mixing under steady-state conditions at ambient temperatures. It should be noted that the steady-state RR conditions used in this study are similar to those of Proshlyakov *et al.* (23). Fig. 3 (*trace g*) shows the high frequency RR spectrum of the Y280H/H_2O_2 reaction. The RR spectra of the oxidized enzyme at pH 6.6 (*trace a*), 7.7

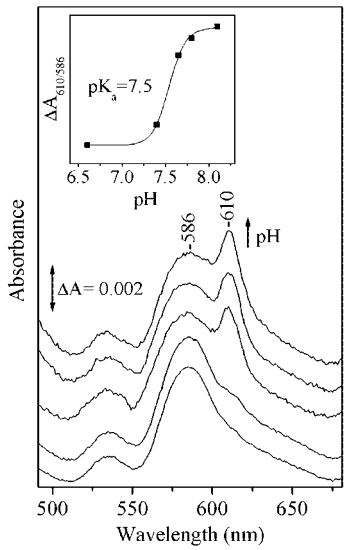

FIG. 2. **pH dependence of the 610- and 586-nm forms of the wild-type aa_3/H_2O_2 reaction at pH 6.6, 7.4, 7.7, 7.8, and 8.1 at 2 min; sample concentration, 6 μM; [H_2O_2] = 3 mM.** The *inset* shows $\Delta A_{610/586}$ as a function of pH. The path length of the cell was 1 cm.

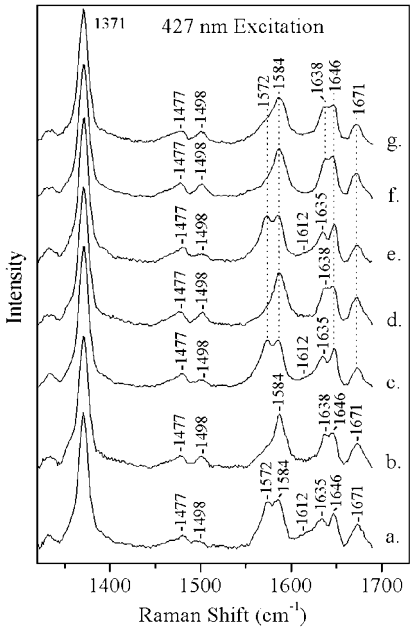

FIG. 3. **High frequency resonance Raman spectra of wild type and those of the reaction intermediates with H_2O_2 at 2 min subsequent to mixing in the pH 6.6–9.6 range.** *Trace a*, pH 6.6; *trace b*, the reaction product at pH 6.6; *trace c*, pH 7.7; *trace d*, the reaction product at pH 7.7; *trace e*, pH 9.6; *trace f*, the reaction product at pH 9.6; *trace g*, the RR spectrum of the Y280H/H_2O_2 reaction at pH 7.7. The concentration of the enzymes was 50 μM, and that of H_2O_2 was 3 mM. The excitation laser wavelength was 427 nm, and the incident laser power was 5–6 milliwatt. The total accumulation time was 15 min for each spectrum.

(*trace c*), and 9.6 (*trace e*) are almost identical, indicating that no unusual pH effects modify either the oxidation state of heme a and a_3 or the heme a_3 ligand binding site. The disappearance of the high spin ν_2 at 1572 cm^{-1} and ν_{10} at 1612 cm^{-1} during the reaction indicates the formation of oxygenated species similar to those reported for the bovine aa_3/H_2O_2 reaction. The absence of ν_2 and ν_{10} at lower frequencies does not support the formation of a porphyrin π-cation radical. In addition, the increased intensity at 1584 cm^{-1} of the ν_2 mode and that of the ν_{10} mode of heme a_3 at 1638 cm^{-1} throughout the pH range

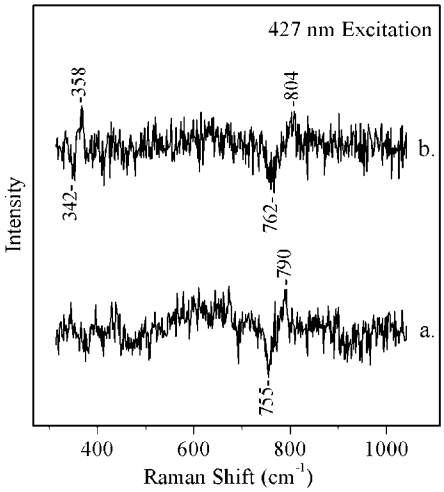

FIG. 4. **Low frequency $H_2{}^{16}O_2/H_2{}^{18}O_2$ RR difference spectra at 2 min in the reaction of oxidized CcO with hydrogen peroxide.** *Trace a* is at pH 6.6 (586-nm form), and *trace b* is at pH 7.7. The concentration of the enzymes was 50 μM, and that of H_2O_2 was 3 mM. The excitation laser wavelength was 427 nm, and the incident laser power was 5–6 milliwatt. The total accumulation time was 35–45 min for each spectrum.

indicate that both the 610- and 586-nm forms are low spin heme a_3 adducts.

All the modes associated with the high spin heme $a_3{}^{3+}$ in the Y280H/H_2O_2 reaction spectrum (*trace g*) are very similar to those of the wild-type enzyme. In particular, the high spin ν_2 at 1572 cm^{-1} and ν_{10} at 1612 cm^{-1} have lost intensity during the reaction, indicating the formation of oxygenated species similar to those reported for the wild-type aa_3/H_2O_2 reaction. The residual high spin ν_2 at 1572 cm^{-1} arises from incompletely reacted heme a_3. Thus, although the reported activity of the Y280H mutant is 1%, only a fraction of heme a_3 (15–20%) is not converted to six-coordinate low spin species in the peroxide reaction. In addition, the substantial heterogeneity observed in the CO-bound fully reduced mutant enzyme that is a consequence of the different conformations of Cu_B is not observed in the peroxide reaction. This is clearly demonstrated by the great similarity in the bandwidth and band position of the ν_2 mode at 1584 and ν_{10} mode at 1638 cm^{-1} in the wild-type (*traces b, d,* and *f*) and Y280H/H_2O_2 (*trace g*) reactions.

In Fig. 4, we present low frequency $H_2{}^{16}O_2/H_2{}^{18}O_2$ RR difference spectra at 2 min in the reaction of oxidized CcO with hydrogen peroxide. *Trace a* shows an oxygen vibration at 790/755 cm^{-1} for $H_2{}^{16}O_2/H_2{}^{18}O_2$ derivatives at pH 6.6 and is the only isotope-sensitive mode present. The frequency, bandwidth, and isotope shift of the 790/755 cm^{-1} mode match closely those observed in the reaction of fully reduced bovine aa_3/O_2 reaction and that of the oxidized CcO with H_2O_2 and have been assigned to a heme a_3 Fe(IV)=O species (30–39). *Trace b* shows the analogous RR spectra at pH 7.7. In this difference spectrum, two more oxygen-sensitive modes appear. The first mode appears at 804/762 cm^{-1}, and the other appears at 358/342 cm^{-1}. Both modes have the same frequency as those observed in the reactions of fully reduced and mixed valence bovine aa_3/O_2 reaction and oxidized CcO with H_2O_2 (13, 30–40). The 804 cm^{-1}mode has been assigned to a second heme a_3 Fe(IV)=O species, and the 358 cm^{-1} mode has been assigned to a His-Fe=O bending mode (23).

DISCUSSION

For the sake of comparison with earlier work, in the following discussion, we ascribe the 608–610- and 586-nm forms we have detected in the reactions of *P. denitrificans* aa_3 with O_2

and H_2O_2 to the species referred to in the literature as having 607-and 580-nm absorbance.

The Origin of the 607- and 580-nm Forms—In the oxidized CcO/H_2O_2 reaction, the formation of the 607-nm form increases in the pH 7.7–8.1 range and depends on the experimental conditions. Its population increases as the pH increases in the protocol used by the present authors and by Fabian and Palmer (24, 26), but not in that used by Proshlyakov *et al.* (23). The latter authors reported that in the pH 7.4–10 range, the population of the 607-nm form decreases at higher pH, and the final distribution of the enzyme between the 607- and 580-nm forms at a given pH depends on the enzyme preparation. The pK_a of ~7.5 we have measured for the 607–580-nm transition is consistent with that reported by Fabian and Palmer (26). However, these authors excluded the involvement of an amino acid residue with a pK_a of ~7.5 being responsible for the 607–580-nm transition. They found that above neutral pH, their enzyme undergoes autoreduction with a rate similar to that of the decay of the 607-nm form, and the rate of autoreduction increases as the pH is raised. We have not observed such autoreduction in the pH 6.6–9.6 range, as is evident in the optical and RR data, and thus, we suggest that the observed transition indeed reflects a pK_a of ~7.5.

A variety of factors are expected to contribute to the differences in absorption maxima between the 607- and 580-nm species. The most likely rationale for the conversion of the 607- to 580-nm form involves the hydrogen-bonding differences in the distal environment and variations in the basicity of the proximal to heme a_3 His-411. The large difference in wavelength maximum for the two forms, 25–30 nm, is unlikely to arise from a change in a single hydrogen-bonding interaction. It has been shown, for example, that the difference in a hydrogen-bonded (pH 7) and non-hydrogen-bonded (pH 11) Fe(IV)=O species in myeloperoxidase is only 7 nm (54). We suggest, instead, that a change in the distal H-bonded environment of the oxoferryl species can be communicated to the proximal environment, causing a modification of the H-bonding status of the proximal heme a_3-His-411. This way, the optical transition will shift to higher energy as a result of the increased splitting of the d orbitals and the energy of the antibonding π^* orbitals. The data for the aa_3-type oxidase from *Bacillus subtilis* (55) show that such heme-linked ionization phenomena exist in heme copper oxidases, which also occur for the peroxidase class of enzymes (56), and are consistent with our interpretation that the effect that comes from the unique interactions between the oxoferryl species and the distal heme pocket environment. Thus, the formation of the 607-nm species can communicate events to the proximal environment, causing perturbations in the H-bonding interactions of His-411.

The general consensus that in the CcO/H_2O_2 reaction, the 607-nm form converts to another form, with a maximum wavelength, which varies between 575 and 593 nm, as a result of changes in the distal hydrogen-bonding interactions, is also consistent with our data (23). Although we detect the 607-nm form in both the wild-type and Y280H mutant enzyme reactions with H_2O_2, we observe a 7-nm red shift for the 580-nm transition in the mutant. It is well established that the tyrosine hydroxyl group is hydrogen-bonded to the farnesyl hydroxyl group of heme a_3 and that the cross-link between Tyr-280 and His-276 exerts a certain control on the position of Cu_B (9, 11, 41). Moreover, the Fourier transform infrared studies of the CO-bound form of the Y280H mutant have demonstrated that in the absence of the cross-link Tyr-His, the heme a_3-Cu_B distance has changed, and Cu_B is not fixed in a certain position, resulting in different Cu_B conformations. Consequently, in the Y280H mutant, Cu_B has moved further closer to the CO-bound heme a_3 and exerts stronger steric force on the bound ligands to heme a_3 (41). We suggest that the 593-nm form is an oxoferryl species, similar to the 586-nm form found in the wild-type but lacking the heterogeneous hydrogen-bonding interactions observed in the wild type. The observed 7-nm red shift in the Y280H mutant is consistent with the observed shift between an H-bonded and a non-H-bonded Fe(IV)=O species.

The data of the Y280H/H_2O_2 and Y280H MV/O_2 reactions demonstrate that the 607-nm form is not linked to the redox properties of Tyr-280 and can be produced without its involvement to form a Fe(IV)=O/Cu_B^{2+}-His-Y$^{\bullet}$ species, as recently proposed (13, 14, 16). It should be noted that Fabian and Palmer (24, 25) reported the formation of 7% of a radical species in the oxidized CcO/H_2O_2 reaction, whereas MacMillan *et al.* (27) reported a yield of 20% for a tyrosine radical species produced in the same reaction. Interestingly, density functional calculations have shown that in the covalent bond between N_ϵ of His-276 and C_ϵ of Tyr-280, the neutral radical of the tyrosine Y$^{\bullet}$ could place the spin density of N_δ of the histidine, and thus, coupling between the copper and the organic radical, Y$^{\bullet}$-Cu(II)$_B$ → Y-Cu$_B$(III) might occur (57). This indicates that in the wild-type enzyme, Tyr-280, which is ideally positioned to act as an acid-base catalyst in both the dioxygen and peroxide reactions, may play a role in the formation of the 607-nm species only if a Y$^{\bullet}$-Cu(II)$_B$ → Y-Cu$_B$(III) structure occurs.

Resonance Raman Assignment of the Intermediates—The assignment of the vibrational modes in cytochrome aa_3 from *P. denitrificans* is well established (41). The high frequency RR spectra reported here demonstrate that in the oxidized form of the enzyme and in the pH 6.6–9.6 range, no autoreduction of either the heme a or the heme a_3 occurs, in contrast to the conclusions reported earlier (26). In the RR spectra of the CcO/H_2O_2 reactions, the spin state marker bands ν_2 and ν_{10} are of particular importance as they indicate the formation of low spin heme a_3 and exclude the formation of a porphyrin π-cation radical. The structural identification of the 607- and 580-nm species during the CcO reaction cycle has been a matter of considerable debate. The properties of the intermediates that appear in the 785–805 cm^{-1} frequency range are complicated, and several interpretations have been presented (13, 22–23, 32–34, 39–40). The formation of the oxoferryl species during the oxidized CcO/H_2O_2 reaction shown in Fig. 4 addresses this issue and demonstrates that the 607-nm form gives rise to an oxoferryl species with a Fe(IV)=O stretching mode at 804 cm^{-1}, in agreement with the results of Kitagawa and co-workers (21–23), and an oxygen isotope-sensitive mode at 358 cm^{-1} (see below). The 586-nm species is a second oxoferryl heme a_3 with a Fe(IV)=O stretching mode at 790 cm^{-1}. This assignment is also in agreement with the results of Kitagawa (21–23). The assignment of the 358 cm^{-1} mode, however, is still controversial. Proshlyakov *et al.* (13) considered the Cu_B-OH structure as a possible candidate for the 358 cm^{-1} mode, and both Kitagawa and co-workers (38) and Rousseau and co-workers (39) have assigned it as a His-Fe=O bending vibration of different distorted His-Fe=O species. Our results indicate that the 358 cm^{-1} mode correlates with the 804 cm^{-1} mode, giving the impression that they originate from the same species. However, based on the existing inconsistencies (38, 39) in the assignment of the 358 cm^{-1} species, we cannot assign it at present. However, we do not observe the 358 cm^{-1} mode concurrently with the 790 cm^{-1} mode, and thus, we conclude, in contrast to the results of Rousseau and co-workers (39), that they arise from different species. In addition, the 358 cm^{-1} mode becomes broader only when D_2O is used as a solvent, and thus, it is highly unlikely that the mode arises from a Cu_B-OH species (34).

The Peroxy and Ferryl Species in the MV/O_2 and Oxidized/H_2O_2 Reactions—The formation of the 607-nm form in both the MV-wild type and MV-Y280H reactions with O_2 and in the wild-type and Y280H reactions with H_2O_2 has a number of important implications. First, it establishes crucial links between the two different reactions. Second, in the 607-nm form, which is one electron more oxidized than the form at 580 nm, the additional oxidizing equivalent must be stored at a site other than heme a_3 or Tyr-280. Alternative structures for the 607-nm form include: 1) Fe(V)=O/Cu_B^{2+}, 2) Fe(IV)=O/Cu_B^{3+}, and 3) Fe(IV)=O/Cu_B^{2+} X$^{\cdot}$ (X$^{\cdot}$ = W$^{\cdot}$ or Y$^{\cdot}$). We do not have evidence other than that related to the Y280H to either confirm or reject the presence of a radical species. However, we demonstrate that the 607-nm form produces the 804 cm^{-1} species and suggest that it arises from a Fe(IV)=O/Cu_B^{3+} species. A Fe(V)=O/Cu_B^{2+} structure has been proposed for the 804 cm^{-1} mode in the CcO/O_2 reaction, and very recently, evidence supporting the +5 valence state in a non-heme Fe has been reported (58). As suggested by Kitagawa and co-workers (59), in the presence of an electron-withdrawing group attached to heme a_3 (formyl), the a_{1u} and a_{2u} level could be lower than the d_{xz} and d_{yz} orbitals. Thus, an electron is taken out of the iron orbital, producing the Fe(V) oxidation state, and the d_{xz} and d_{yz} orbitals may act as antibonding orbitals of the Fe=O bond. Consequently, removal of this electron raises the stretching frequency of the Fe(V)=O as compared with the Fe(IV)=O frequency. This can account for the appearance of the Fe(V)=O at 804 cm^{-1} and the Fe(IV)=O at 790 cm^{-1}. The observation of the 805 cm^{-1} mode in the cytochrome bo_3/H_2O_2 reaction (60), however, argues against this possibility since the heme O lacks a strong electron-withdrawing peripheral substituent (61). On the other hand, the occurrence of Cu^{3+} has been demonstrated in model compounds, but supporting evidence in Cu-containing enzymes has not been reported so far (62, 63). Given that a small percentage of radical species has been detected when the 607-nm form was produced, we cannot exclude that a radical species is located in the protein nor the possibility that Cu_B may be in a Y$^{\cdot}$-Cu(II)$_B$ → Y-Cu_B(III) equilibrium intermediate state. If the latter scenario is correct, then the mechanism for the critical O-O scission will be dependent on the equilibrium of Y$^{\cdot}$-Cu(II)$_B$ → Y-Cu_B(III).

The vibrational properties of oxygenated intermediates in histidine-containing peroxidase catalysis have been explained by the push-pull reaction mechanism (64, 65) in which the distal histidine acts as a base to accelerate the binding of H_2O_2 by deprotonating the substrate to give a Fe^{3+}-O-O-R species. The pull aspect of the mechanism involves donation of a proton to the terminal oxygen of the hydroperoxide by the same residue acting as an acid. Concurrently, in the push component of the mechanism, an amino acid in the proximal pocket hydrogen-bonds to the proximal histidine and imparts significant anionic character to this residue. In the absence of Tyr-280 in the distal site, Glu-278 or a deprotonated Cu_B-histidine can play a role as a general acid-base catalyst. It is noteworthy that the involvement of Glu as an acid-base catalyst has been demonstrated in chloroperoxidases where Glu-186 is located at the position corresponding to the distal histidine of horseradish peroxidase (66, 67). Similarly, the basicity of the proximal His-411 can be significantly enhanced by local protein forces and can explain the observed structural differences between the two oxoferryl species we observe at 790 and 804 cm^{-1}. This interpretation finds support from earlier RR studies in which it has been shown that the properties of the trans ligand of oxoferryl complexes can affect the bonding between the iron and the oxygen, and thus, can affect its vibrational frequency (68); the vibrational frequency decreases as the ligand becomes more electron-donating to Fe(IV)=O. Along these lines, a high Fe-His mode arises from a population in which the hydrogen bond is intact, whereas a lower frequency of the Fe-His vibration reflects a form of the enzyme lacking the hydrogen bond (55). Based on the crystal structure, the proximal His-411 is capable of forming a hydrogen bond with Gly-378, and thus, the H-/non H-bonding interaction of the proximal His-411 with Gly-378 is the most likely contributor to the vibrational differences between the two oxoferryl species.

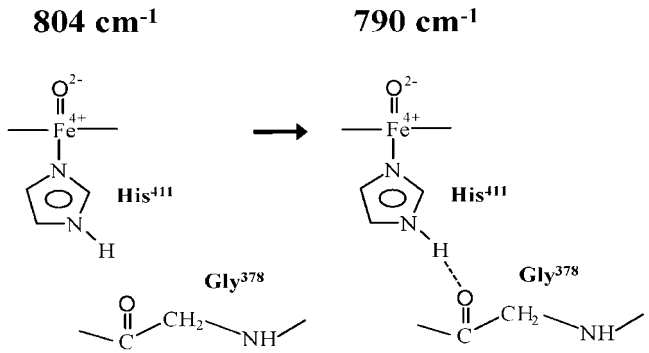

FIG. 5. **Structure-function model of the His-Fe(IV)=O species.**

The disparity in the Fe(IV)=O frequency of the oxoferryl species we have detected is illustrated in Fig. 5. The 804 cm^{-1} species represents a His-Fe(IV)=O structure in which the proximal His-411 is not hydrogen-bonded to Gly-378. We postulate that conformational changes of the 804 cm^{-1} Fe(IV)=O species by the heme a_3/Cu_B pocket are communicated to the proximal environment, as has been observed in the peroxidase class of enzymes, to facilitate the H-bonding interaction of the proximal His-411, producing the 790 cm^{-1} species. In the presence of an H-bonded His-411, electron density is pushed into the antibonding π^* orbitals of Fe(IV)=O, weakening the bond, and thus, shifting the Fe(IV)=O stretching frequency from 804 to 790 cm^{-1}. The details on how the 804–790 cm^{-1} oxoferryl transition is specifically tuned to initiate the H-bonding interaction and whether it is coupled to the heme a_3-propionates-Asp-H_2O protonic connectivity, in a similar manner to that found in cytochrome ba_3 from *T. thermophilus* (69), remain to be determined.

REFERENCES

1. Wikström, M. (1989) *Nature* **338,** 776–778
2. Babcock, G. T., and Wikström, M. (1992) *Nature*, **356,** 301–309
3. Michel, H. (1998) *Proc. Natl. Acad. Sci. U. S. A.* **95,** 12819–12824
4. Michel, H., Behr, J., Harrenga, A., and Kannt, A. (1998) *Annu. Rev. Biophys. Biomol. Struct.* **27,** 329–356
5. Ferguson-Miller, S., and Babcock, G. T. (1996) *Chem. Rev.* **96,** 2889–2907
6. Gennis, R. B. (1998) *Biochim. Biophys. Acta* **1365,** 241–248
7. Tsukihara, T., Aoyama, H., Yamashita, E., Tomizaki, T., Yamaguchi, H., Shinzawa-Itoh, K., Nakashima, R., Yaono, R., and Yoshikawa, S. (1995) *Science* **269,** 1069–1074
8. Soulimane, T., Buse, G., Bourenkov, G. P., Bartunik, H. D., Huber, R., and Than, M. E. (2000) *EMBO J.* **19,** 1766–1776
9. Yoshikawa, S., Shinzawa-Itoh, K., Nakashima, R., Yaono, R., Yamashita, E., Inoue, N., Yao, M., Fei, M. J., Libeu, C. P., Mizushima, T., Yamaguchi, H., Tomizaki, T., and Tsukihara, T. (1998) *Science* **280,** 1723–1729
10. Iwata, S., Ostermeier, C., Ludwig, B., and Michel, H. (1995) *Nature* **376,** 660–669
11. Ostermeier, C., Harrenga, A., Ermler, U., and Michel, H. (1997) *Proc. Natl. Acad. Sci. U. S. A.* **94,** 10547–10553
12. Fabian, M., Wong, W. W., Gennis, R. B., and Palmer, G. (1999) *Proc. Natl. Acad. Sci. U. S. A.* **96,** 13114–13117
13. Proshlyakov, D. A., Pressler, M. A., and Babcock, G. T. (1998) *Proc. Natl. Acad. Sci. U. S. A.* **95,** 8020–8025
14. Michel, H. (1999) *Biochemistry* **38,** 15129–15140
15. Kannt, A., Lancaster, C. R. D., and Michel, H. (1998) *Biophys. J.* **74,** 708–721
16. Proshlyakov, D. A., Pressler, M. A., Demaso, C., Leykam, J. F., DeWitt, D. L., and Babcock, G. T. (2000) *Science* **290,** 1588–1591
17. Wrigglesworth, J. M. (1984) *Biochem. J.* **217,** 715–719
18. Vygodian, T. V., and Konstantinov, A. A. (1988) *Ann. N. Y. Acad. Sci.* **550,** 124–138
19. Konstantinov, A. A., Capitanio, N., Vygodina, T. V., and Papa, S. (1992) *FEBS Lett.* **312,** 71–74

20. Weng. L. C., and Baker, G. M. (1991) *Biochemistry* **30,** 5727–5733
21. Proshlyakov, D. A., Ogura, T., Shinzawa-Itoh, K., Yoshikawa, S., Appelman, E. H., and Kitagawa, T. (1994) *J. Biol. Chem.* **47,** 29385–29388
22. Proshlyakov, D. A., Ogura, T., Shinzawa-Itoh, K., Yoshikawa, S., and Kitagawa, T. (1996) *Biochemistry* **35,** 76–82
23. Proshlyakov, D. A., Ogura, T., Shinzawa-Itoh, K., Yoshikawa, S., and Kitagawa, T. (1996) *Biochemistry* **35,** 8580–8586
24. Fabian, M., and Palmer, G. (1995) *Biochemistry* **34,** 13802–13810
25. Fabian, M., and Palmer, G. (1999) *Biochemistry* **38,** 6270–6275
26. Fabian, M., and Palmer, G. (2001) *Biochemistry* **40,** 1867–1874
27. MacMillan, F., Kannt, A., Behr, J., Prisner, T., and Michel, H. (1999) *Biochemistry* **38,** 9179–91884
28. Rigby, S. E. J., Jünemann, S., Rich, P. R., and Heathcote, P. (2000) *Biochemistry* **39,** 5921–5928
29. Verkhovsky, M. I., Morgan, J. E., and Wikström, M. (1996) *Proc. Natl. Acad. Sci. U. S. A.* **93,** 12235–12239
30. Varotsis, C., and Babcock, G. T. (1990) *Biochemistry* **32,** 7357–7362
31. Ogura, T., Takahashi, S., Hirota, S., Shinzawa-Itoh, K., Yoshikawa, S., and Kitagawa, T. (1990) *J. Biol. Chem.* **265,** 14721–14723
32. Han, S., Ching, Y.-C., and Rousseau, D. L. (1990) *Nature* **348,** 89–90
33. Ogura, T., Takahashi, S., Shinzawa-Itoh, K., Yoshikawa, S., and Kitagawa, T. (1990) *J. Am. Chem. Soc.* **112,** 5630–5631
34. Varotsis, C., Zhang, Y., Appelman, E. H., and Babcock, G. T. (1993) *Proc. Natl. Acad. Sci. U. S. A.* **90,** 237–241
35. Ogura, T., Takahashi, S., Hirota, S., Shinzawa-Itoh, K., Yoshikawa, S., Appleman, E. H., and Kitagawa, T. (1993) *J. Am. Chem. Soc.* **115,** 8527–8536
36. Ogura, T., Takahashi, S., Hirota, S., Shinzawa-Itoh, K., Yoshikawa, S., Appleman, E. H., and Kitagawa, T. (1994) *J. Biol. Chem.* **269,** 29385–29388
37. Varotsis, C., Lauraeus, M., Babcock, G. T., and Wikström, M. (1995) *Biochim. Biophys. Acta* **1231,** 111–116
38. Ogura, T., Hirota, S., Proshlyakov, D. A., Shinzawa-Itoh, K., Yoshikawa, S., and Kitagawa, T. (1996) *J. Am. Chem. Soc.* **118,** 5443–5449
39. Han, S., Takahashi, S., and Rousseau, D. L. (1999) *J. Biol. Chem.* **275,** 1910–1919
40. Kim, Y., Shinzawa-Itoh, K., Yoshikawa, S., and Kitagawa, T. (2001) *J. Am. Chem. Soc.* **123,** 757–758
41. Pinakoulaki, E., Pfitzner, U., Ludwig, B., and Varotsis, C. (2002) *J. Biol. Chem.* **277,** 13563–13568
42. Hendler, R. W., Pardhasaradhi, K., Reynafarje, B., and Ludwig, B. (1991) *Biophys. J.* **60,** 415–423
43. Pfitzner, U., Odenwald, A., Ostermann, T., Weingard, L., Ludwig, B., and Richter, O.-M. H. (1998) *J. Bioenerg. Biomembr.* **30,** 89–97
44. Varotsis, C., Oertling, W., and Babcock, G. T., (1990) *Appl. Spectrosc.* **44,** 742–746
45. Varotsis, C., Woodruff, W. H., and Babcock, G. T. (1989) *J. Am. Chem. Soc.* **111,** 6439–6440
46. Varotsis, C., Woodruff, W. H., and Babcock, G. T. (1990) *J. Biol. Chem.* **265,** 11131–11136
47. Varotsis, C., and Babcock, G. T. (1995) *J. Am. Chem. Soc* **117,** 11260–11269
48. Varotsis, C., and Babcock, G. T. (1993) in *Methods in Enzymology, Metalobiochemistry, Part C*, (Riordan J. F., and Vallee, B. L., eds) pp. 409–431, Academic Press, Orlando, FL
49. Vygodina, T. V., Pecoraro, C., Mitchell, D., Gennis, R., and Konstantinov, A. A. (1998) *Biochemistry* **37,** 3053–3061
50. Pecoraro, C., Gennis, R. B., Vygodina, T. V., and Konstantinov, A. A. (2001) *Biochemistry* **40,** 9695–9708
51. Morgan, J. E., Verkhovsky, M. I., Palmer, G., and Wikström, M. (2001) *Biochemistry* **40,** 6882–6892
52. Einarsdóttir, Ó, Szundi, I., van Eps, N., and Sucheta, A. J. (2002) *J. Inorg. Biochem.* **91,** 87–93
53. Han, S., Ching, Y.-C., and Rousseau, D. L. (1990) *J. Am. Chem. Soc.* **112,** 9445–9451
54. Oertling, W. A., Hoogland, H., Babcock, G. T., and Weaver, R. (1988) *Biochemistry* **27,** 5395–5400
55. Varotsis, C., and Vamvouka, M. (1998) *J. Phys. Chem. B* **102,** 7670–7673
56. Hayashi, Y., and Yamazaki, I. (1978) *Arch. Biochem. Biophys.* **190,** 446–453
57. Palmer, G. (1998) *EBEC Short Rep.* **10,** 85
58. Bassan, A., Blomberg, M. R. A., Siegbahn, P. E. M., and Que, L., Jr. (2002) *J. Am. Chem. Soc.* 124, 11056–11063
59. Kitagawa, T. (2000) *J. Inorg. Biochem.* **82,** 9–18
60. Uchida, T., Mogi, T., Kitagawa, T. (2000) *Biochemistry* **39,** 6669–6678
61. Wu, W., Varotsis, C., Babcock, G. T., Chang, C. K., Puustinen, A., and Wikström, M. (1992) *J. Am. Chem. Soc.* **114,** 1182–1188
62. McDonald, M. R., Fredricks, F. C., and Margerum, D. W. (1997) *Inorg. Chem.* **36,** 3119–3124
63. McDonald, M. R., Scheper, W. H., Lee, H. D., and Margerum, D. W. (1995) *Inorg. Chem.* **34,** 229–237
64. Poulos, T. L. (1987) *Adv. Inorg. Biochem.* **7,** 1
65. Dawson, J. H. (1988) *Science* **240,** 433–439
66. Sundaramoorthy, M., Terner, J., and Poulos, T. L. (1995) *Structure* **3,** 1367–1377
67. Hashimoto, S., Tatsuno, Y., and Kitagawa, T. (1986) *Proc. Natl. Acad. Sci. U. S. A.* **83,** 2417–2421
68. Oertling, W. A., Kean, R. T., Wever, R., and Babcock, G. T. (1990) *Inorg. Chem.* **29,** 2633–2645
69. Koutsoupakis, K., Stavrakis, S., Pinakoulaki, E., Soulimane, T., Varotsis, C. (2002) *J. Biol. Chem.* **277,** 32860–32866
70. Varotsis, C., Woodruff, W. H., and Babcock, G. T. (1989) *J. Am. Chem. Soc.* **112,** 1297